4. Water Vapor Patterns

4.1. Introduction

In water vapor imagery, airflow in upper and middle tropospheric layers can be visualized using water vapor as a tracer, even in the absence of clouds. The positions of troughs, ridges, vortices and jet streams in these layers can be estimated from bright and dark patterns in such imagery, as well as trough deepening from temporal changes in bright and dark patterns. However, the imagery provides little information about the lower troposphere due to strong absorption by water vapor.

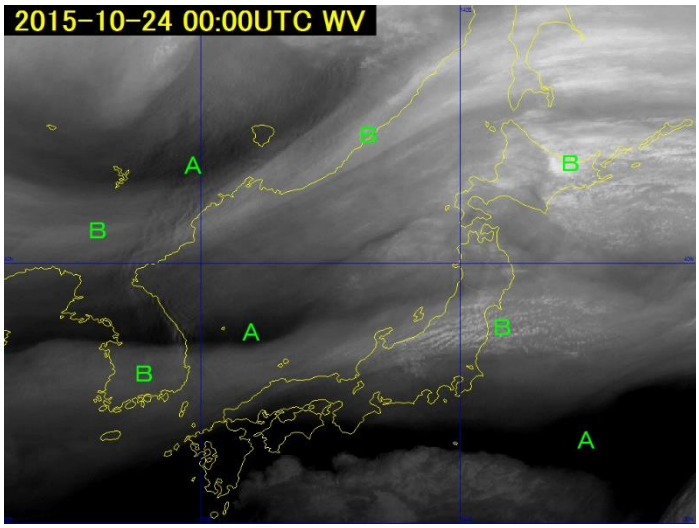

Fig. 4-1-1 Water vapor image for 00:00 UTC on 24 October 2015

4.1.1. Dark Regions

Relatively dark areas in water vapor imagery are called dark regions, which have high brightness temperature indicating dry upper and middle troposphere layers. Each water vapor band has a different sensitive altitude. Areas with **A** in Fig. 4-1-1 are dark regions.

4.1.2. Bright Regions

Relatively bright areas in water vapor imagery are called bright regions, which have low brightness temperature indicating humid upper and middle troposphere layers or cloud areas with tops in the upper and middle troposphere. Areas with **B** in Fig. 4-1-1 are bright regions. Dark and bright regions are determined qualitatively rather than quantitatively.

4.1.3. Darkening

Darkening is a phenomenon in which the darkness of areas increases over time. Darkening regions correspond to active subsidence fields, indicating trough deepening and anticyclone strengthening. Comparison of areas with **C** in Figs. 4-1-2 and 4-1-3 shows darkening.

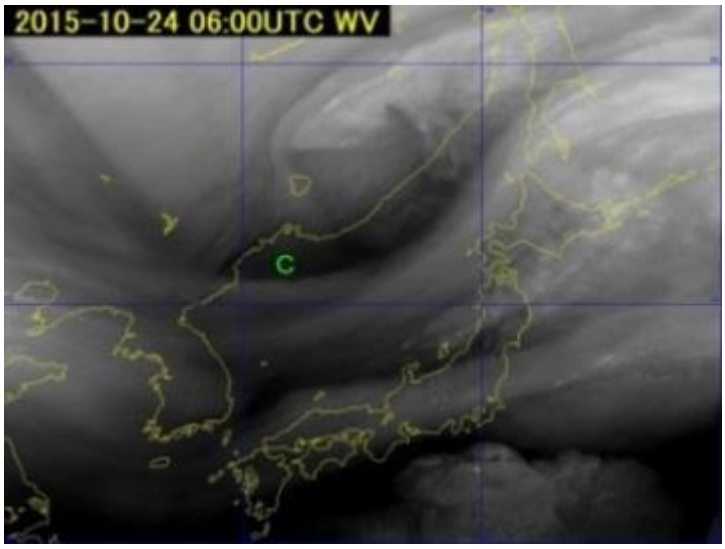

Fig. 4-1-2 Water vapor image for 06:00 UTC on 24 October 2015

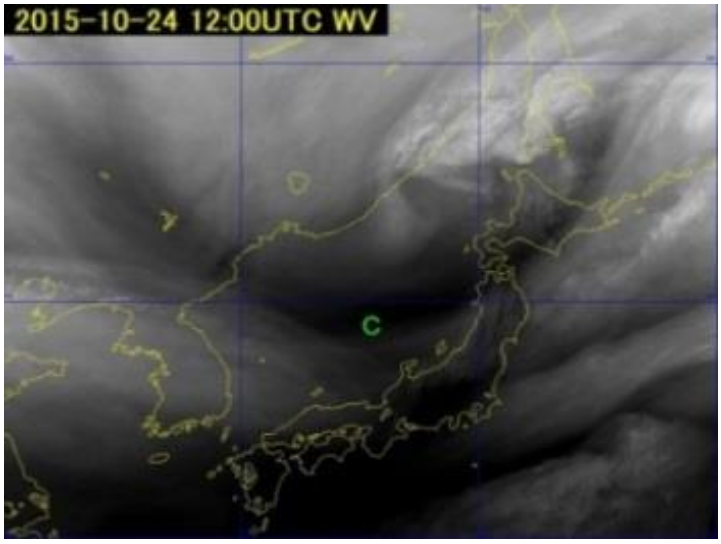

Fig. 4-1-3 Water vapor image for 12:00 UTC on 24 October 2015

4.1.4. Dry Intrusion

The descent of extremely dry air into lower layers near a cyclone is called dry intrusion. In water vapor imagery, descending dry air masses appear as clear dark or darkening regions, highlighting the development of dry intrusion. Browning (1999) emphasizes that such intrusion affects the structure of extratropical cyclone fronts, clouds and precipitation because the dry air mass descends from near the tropopause with low potential temperature, and is associated with convective instability and the occurrence of convection. The descending mass is separated at the rear of a cold front into flow toward the cyclone center and anticyclonic flow. This may produce a dark region with a hammerhead pattern in water vapor imagery (Fig. 4-1-4).

Figure 4-1-5 shows a dry intrusion, with a belt-form dark region heading from the northwest to a cyclone near Mongolia. The intrusion separates at the rear of the cyclone, with one part heading toward the cyclone center and the other west-southwestward around 40°N, with a hammerhead pattern.

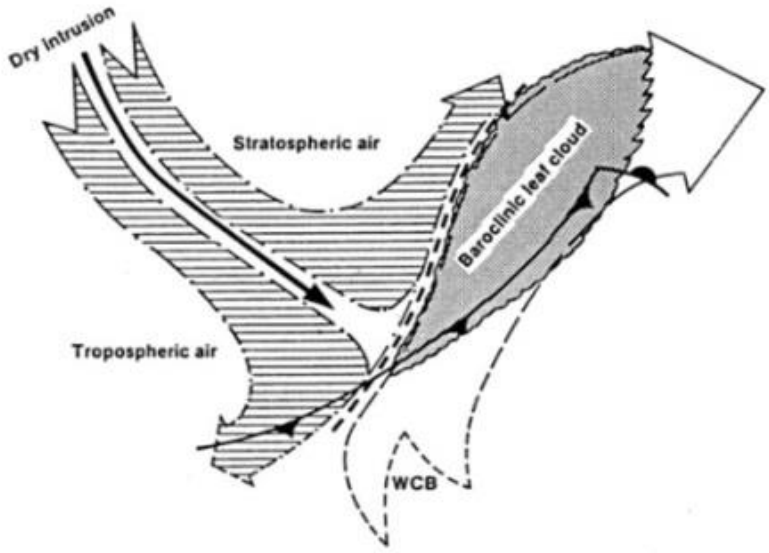

Fig. 4-1-4 Dry intrusion with a hammerhead pattern (Young *et al.,* 1987)

4.1.5. Dry Slots

Dry air masses flowing from a cold air mass side toward a developing cyclone center are called dry slots. In water vapor imagery, these appear as dark regions resembling narrow grooves around the cyclone center. In visible and infrared imagery, they appear as cloudless or lower-cloud areas. Dry slots are formed by dry intrusions.

In the dry slot shown in Figs. 4-1-5 and 4-1-6, there is a thin dark region around the cyclone center (arrow) at the cyclone center near Mongolia, forming a partial hammerhead pattern. In visible imagery, this is a mostly clear-sky area.

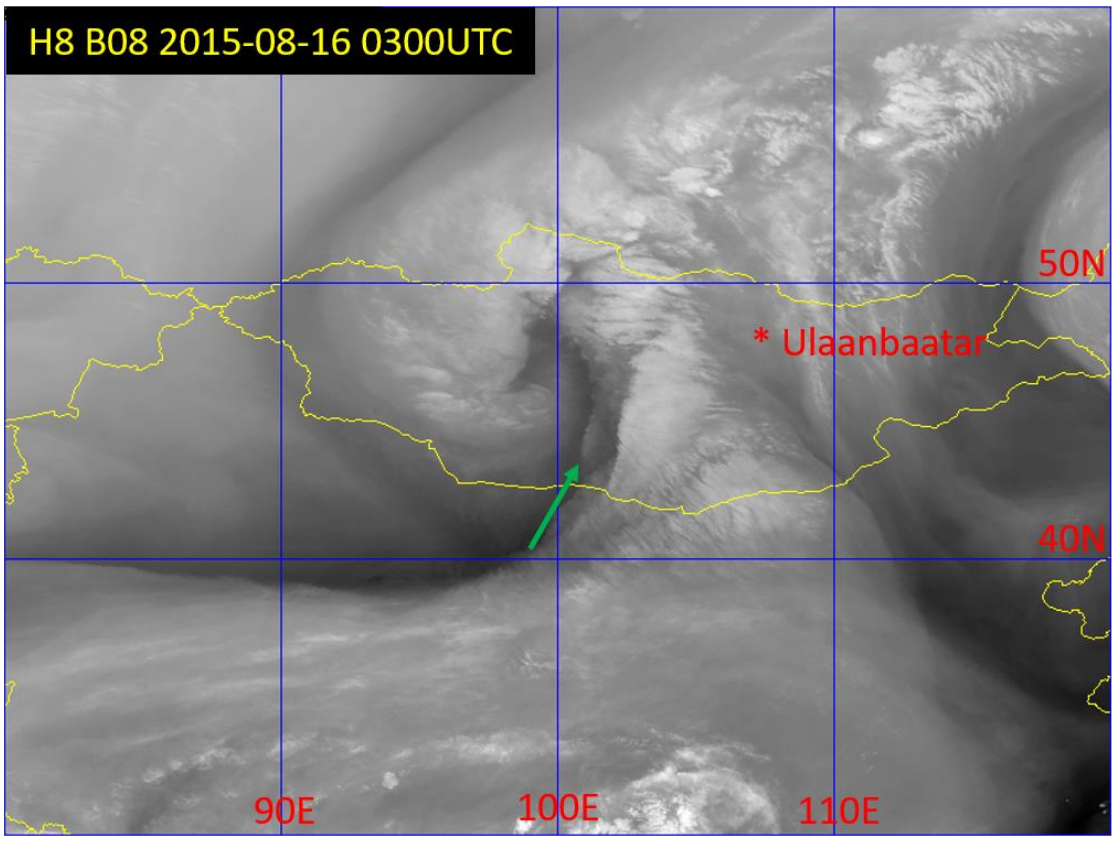

Fig. 4-1-5 Water vapor image of a dry intrusion for 03:00 UTC on 16 August 2015. Green arrow: dry slot.

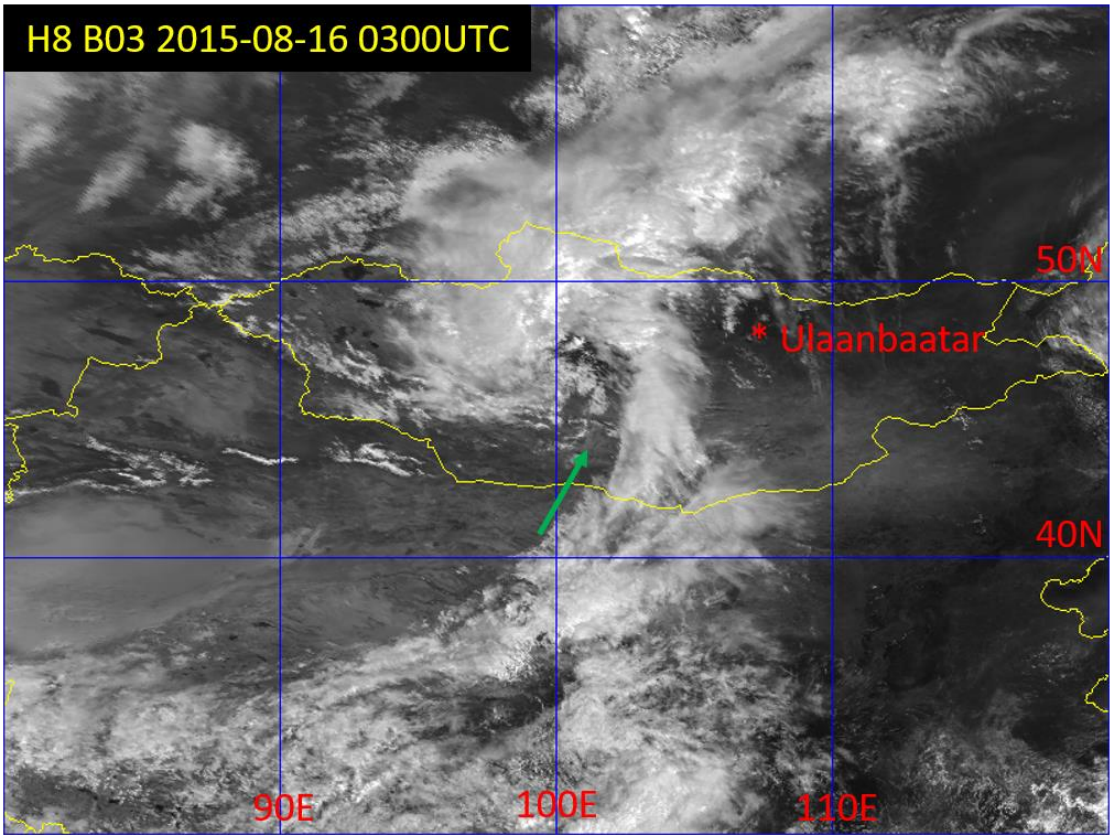

Fig. 4-1-6 Visible image of a dry intrusion for 03:00 UTC on 16 August 2015. Green arrow: dry slot.

4.1.6. Upper Troughs

Using water vapor imagery, upper troughs can be seen at the maximum cyclonic curvature of a boundary between bright and dark regions (i.e., a dark region with a convex shape to the south; Fig. 4-1-7). Troughs in the upper and middle layers can be determined from the boundary shape, and trough deepening can be estimated from the degree of darkening. From Fig. 4-1-8, a trough over Northeast China can be seen from the boundary curvature and from GSM 500 hPa contour lines.

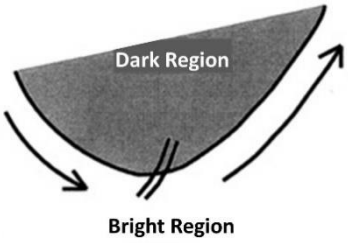

Fig. 4-1-7 Upper trough

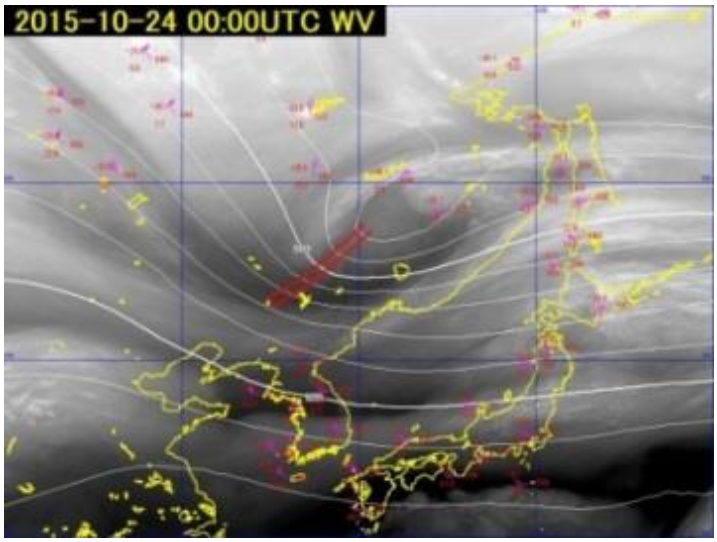

Fig. 4-1-8 Water vapor image for 00:00 UTC on 24 October 2015.
White lines: contours every 60 m (geopotential height) at 500 hPa from GSM data; red double line: upper trough.

4.1.7. Upper Vortices

Vortices can be identified from temporal changes in water vapor imagery showing spirals of bright and dark regions and their rotation. Those identifiable in such imagery are called upper vortices, which are useful for detecting cyclones and troughs in upper and middle troposphere layers. Figure 4-1-9 shows an upper vortex (arrow) identifiable from the spiral of bright and dark regions.

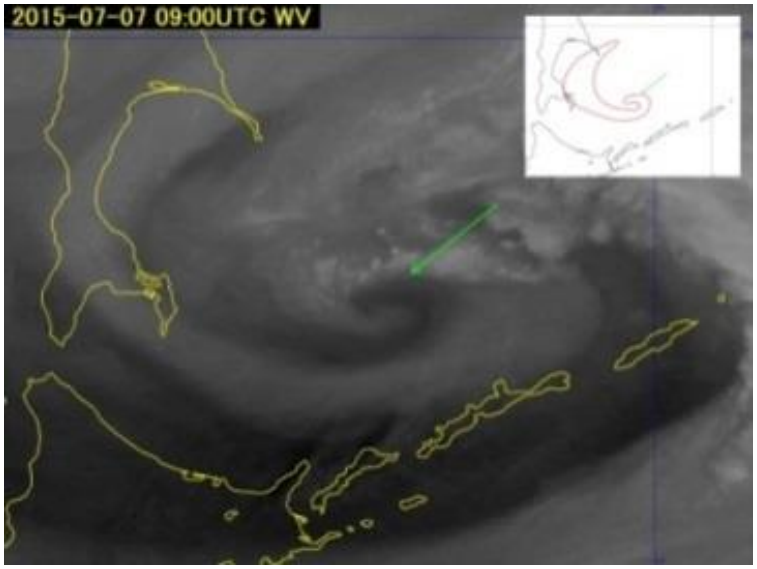

Fig. 4-1-9 Water vapor image for 09:00 UTC on 7 July 2015, showing an upper vortex (green arrow).

Reference

- Young *et al.,* 1987: Interpretation of Satellite Imagery of A Rapidly Deepening Cyclone, Quarterly Journal of the Royal Meteorological Society 113 (478), 1089-1115,

4.2. Boundaries

Borders between bright and dark regions in water vapor imagery are called boundaries. These represent divisions between air masses with different moisture levels in the upper and middle layers, therefore appearing clearly when the spatial gradient of moisture is significant. Boundaries are formed by vertical flow and horizontal deformation of the atmosphere, each exhibiting a characteristic pattern.

Weldon and Holmes (1991) classify boundaries into seven types (Table 4-2-1) and describe their characteristics (including those related to jet streams, those exhibiting blocking, and those exhibiting surges) based on causes and structures. The type of boundary can change both temporally and spatially, such as when transitioning from a base surge boundary to an inside boundary and when the upstream part of the boundary is a dry surge type but the downstream part is a baroclinic leaf type. This section outlines the boundary types classified by Weldon and Holmes (1991).

Table 4-2-1 Classification of boundaries (Weldon and Holmes, 1991)

Boundary related to jet stream	Parallel jet stream boundary
	Baroclinic leaf boundary
Boundary exhibiting a blocking	Head boundary
	Inside boundary
Boundary exhibiting a surge	Dry surge boundary
	Base surge boundary
Others	Return moisture boundary

4.2.1. Boundaries Related to Jet Streams

One of the most effective uses of water vapor imagery involves observation of changes in jet streams. Air masses to the poles of the jet stream are generally cold and dry, while those to the equator are warm and humid. A boundary appears when the cloud area corresponding to the front brightens.

Figure 4-2-1 illustrates subtropical and polar frontal zones (Ramond *et al.,* 1981). Subsidence strengthens on the pole side above the frontal zone near the jet, and a dry region hangs down from the tropopause. The dark region to the north of the jet corresponds to this region and forms a boundary with clear contrast. Subtropical frontal zones are generally wide and steep, tending to form wider and clearer boundaries than polar frontal zones.

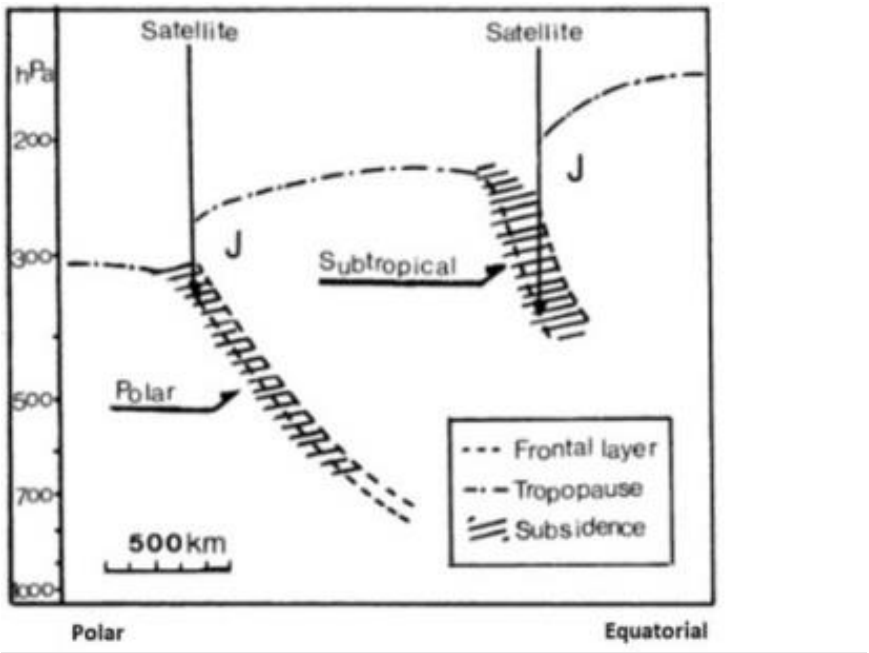

Fig. 4-2-1 Schematic drawing of subtropical and polar frontal zones (Ramond *et al.,* 1981)

4.2.1.1. Parallel Jet Stream Boundaries

Parallel jet stream boundaries form at the border between cloud areas (bright) accompanying jet streams and dark regions on the polar side (Fig. 4-2-2). These often exhibit sharp contrast and quasi-linear shapes. Dark regions often appear as bands on the polar side of the jet stream. The positions of the jet axis and the boundary often coincide, but in the westerly wind zone, the western edge of the jet axis is often in the deformation field. Accordingly, the shape and contrast of the boundary may be less clear than those of the eastern edge, or may not coincide with the jet axis.

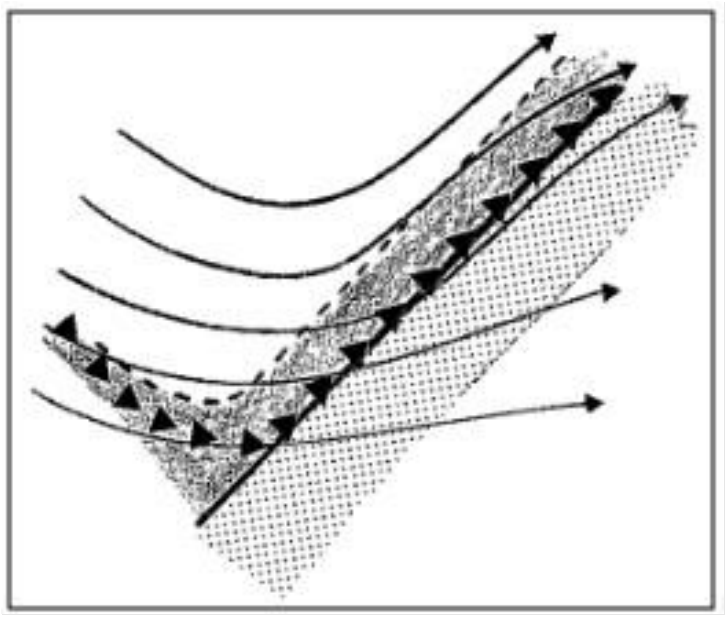

Fig. 4-2-2 Schematic illustration of a parallel jet stream boundary. Shading: dark region;

white: bright region; dotted area: cloud; thick line: boundary; thin arrows: streamlines; black triangles: axis of maximum wind speed.

Figure 4-2-3 shows a parallel jet stream boundary. There is clear boundary from the coast of San'in to the coast of Akita, which coincides with the jet stream core at around 80 kt. The boundary extends from the San'in region through northern Kyushu to East China, but since northern Kyushu is located at the inlet to the jet core, correspondence between the boundary and the jet axis is unclear.

In Fig. 4-2-3, the area that can be identified as a parallel jet stream boundary in front of a clear trough is less than 1,000 km. Conversely, in Fig. 4-2-4, a clear parallel jet stream boundary extends at least 4,000 km from the area near the Yellow Sea to around 180° longitude.

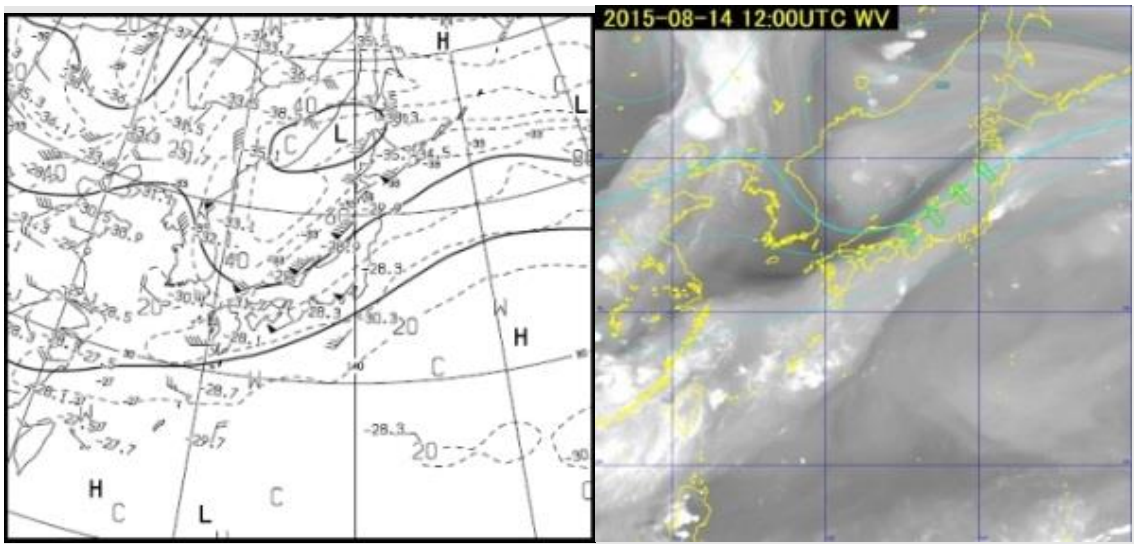

Fig. 4-2-3 Parallel jet stream boundary for 12:00 UTC on 14 August 2015. Left: 300 hPa weather chart; right: water vapor image; green arrows: boundary.

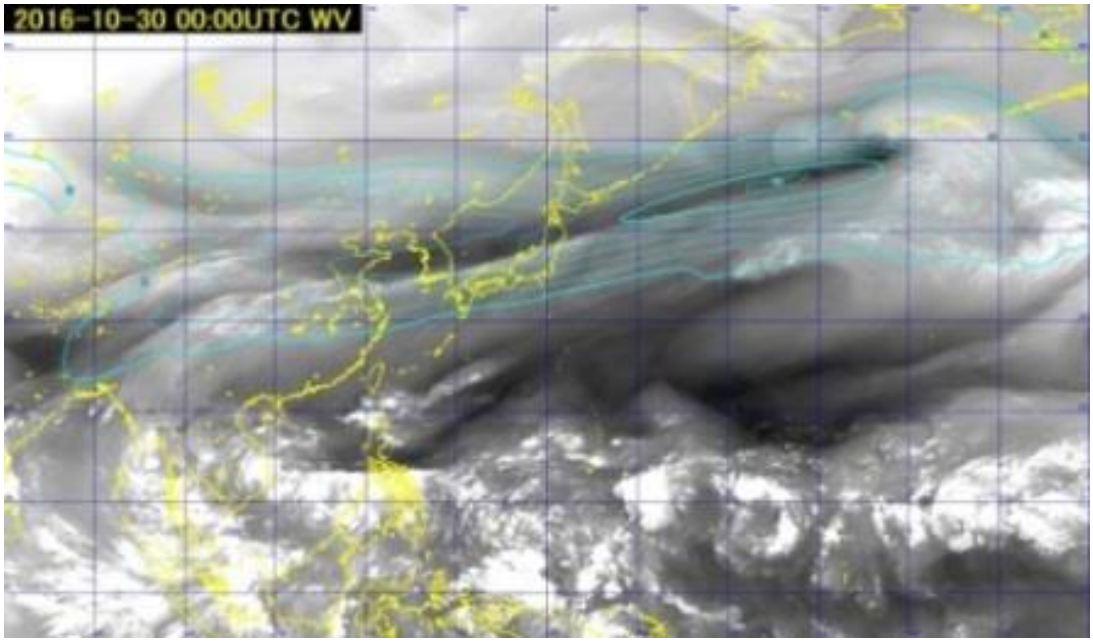

Fig. 4-2-4 Water vapor image for 00:00 UTC on 30 October 2016, showing a parallel jet stream boundary. Cyan lines: isotachs (60 kt or more, every 20 kt) at 300 hPa from GSM.

4.2.1.2. Baroclinic Leaf Boundaries

Baroclinic leaf boundaries are also related to jet streams, and are accompanied by leaf-shaped cloud areas (cloud leaves) that appear at the early stage of cyclogenesis in the westerly wind belt. Due to the warm conveyor belt (WCB; Section 5.1), which is a warm and humid current in the early stage of cyclogenesis, the cloud area forms a leaf pattern in front of the trough, as shown in Fig. 4-2-5, and the boundary exhibits an S-shape. Generally, the side of the S-shape where the bright region bulges toward the poles is parallel to the jet axis, while the other side (where the dark region bulges toward the tropics) is closer to the deformation field and may not be parallel to the jet axis.

Figure 4-2-6 presents a baroclinic leaf boundary. To the west of the Bohai Sea, there is a leaf-shaped cloud area corresponding to a developing cyclone. Its northern edge has an anticyclonic curvature and is aligned with the jet axis. Baroclinic leaf boundaries are often formed where jets converge.

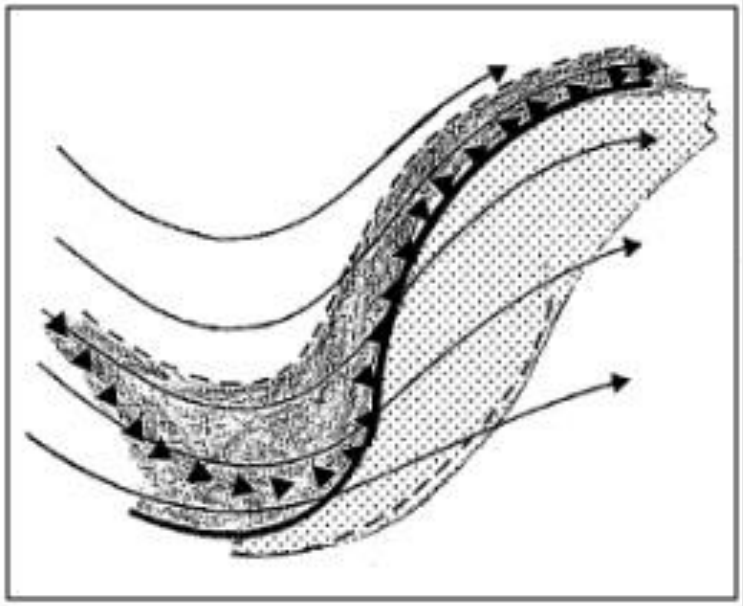

Fig. 4-2-5 Schematic illustration of a baroclinic leaf boundary. Shading: dark region; white: bright region; dotted area: cloud; thick line: boundary; thin arrows: streamlines; black triangles: axis of maximum wind speed.

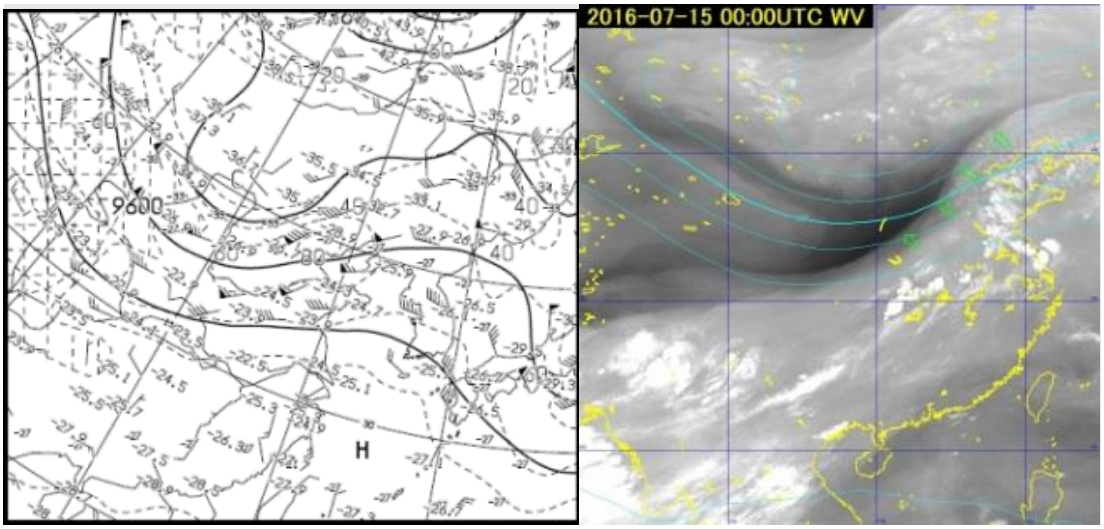

Fig. 4-2-6 Baroclinic leaf boundary for 00:00 UTC on 15 July 2016. Left: 300 hPa weather chart; right: water vapor image; green arrows: boundary.

4.2.2. Boundaries Exhibiting Blocking

This type of boundary is formed by the development of circulation with a wind field in the opposite direction to the surrounding wind in an area with relatively weak upper-level wind. As a circulation field that blocks the surrounding wind is formed in such cases, the phenomenon is referred to as a boundary exhibiting blocking. Based on the origin of the circulation field, these can be divided into head boundaries related to cyclone formation, and inside boundaries related to anticyclone formation.

4.2.2.1. Head Boundaries

Head boundaries are borders between convex bright regions and surrounding dark regions. This type moves and changes slowly, and is formed by synoptic-scale streams associated with cyclogenesis. As per Fig. 4-2-7, cyclones cause moist air masses to rise from the lower layer and form a head-shaped bright region divided into a stream along the cyclone and an anticyclonic flow north of the cyclone. The stream in the bright region is blocked by surrounding dry westerly winds and becomes a downward stream at the border. In the field of the upper stream, a boundary is formed along the elongation axis of the deformation field.

Figure 4-2-8 shows a head boundary. A clear boundary is seen over the sea south of the Kamchatka Peninsula at the border between easterly wind associated with cyclonic circulation east of the Kuril Islands and northwesterly wind from the Sea of Okhotsk at 300 hPa. The presence and scale of upper cyclones, which are difficult to judge from weather charts alone, can be estimated from boundaries.

Fig. 4-2-7 Schematic illustration of a head boundary. Shading: dark region; white: bright region; thick line: boundary; thin arrows: streamlines; black triangles: axis of maximum wind speed.

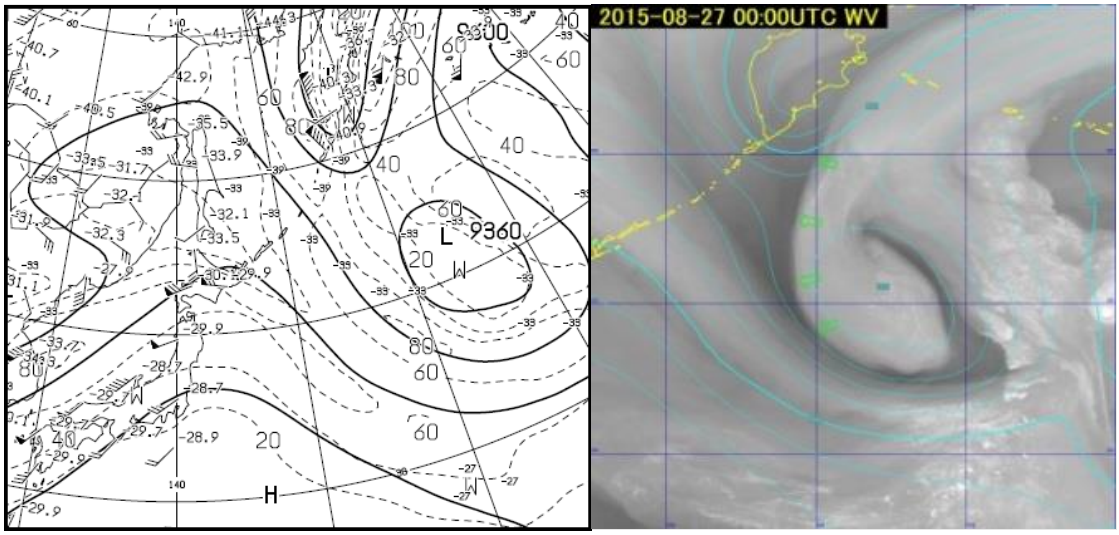

Fig. 4-2-8 Head boundary for 00:00 UTC on 27 August 2015. Left: 300 hPa weather chart; right: water vapor image; green arrows: boundary, cyan lines: 300 hPa contour line from GSM.

4.2.2.2. Inside Boundaries

As subsidence due to anticyclones in the upper layer causes dry areas to form and spread, a border is formed between the dry area and any relatively wet current alongside an upper trough. Such borders formed by anticyclonic circulation are called inside boundaries. As per Fig. 4-2-9, these form between convex dark regions toward the upstream side and surrounding bright areas. This type moves and changes slowly, and can be used to monitor the degree of development and movement of blocking anticyclones.

Figure 4-2-10 shows an inside boundary. A vortex corresponding to an upper cyclone can be seen near Primorye, while a ridge in the opposite phase can be seen to the north. This is difficult to understand from the 300 hPa weather chart (Fig. 4-2-10) alone, but the contours on the water vapor image suggest an upper anticyclone extending westward from northern Sakhalin at the north of the upper cyclone. An inside boundary is formed between this anticyclonic stream and the moist westerly wind (bright region) in front of the trough upstream.

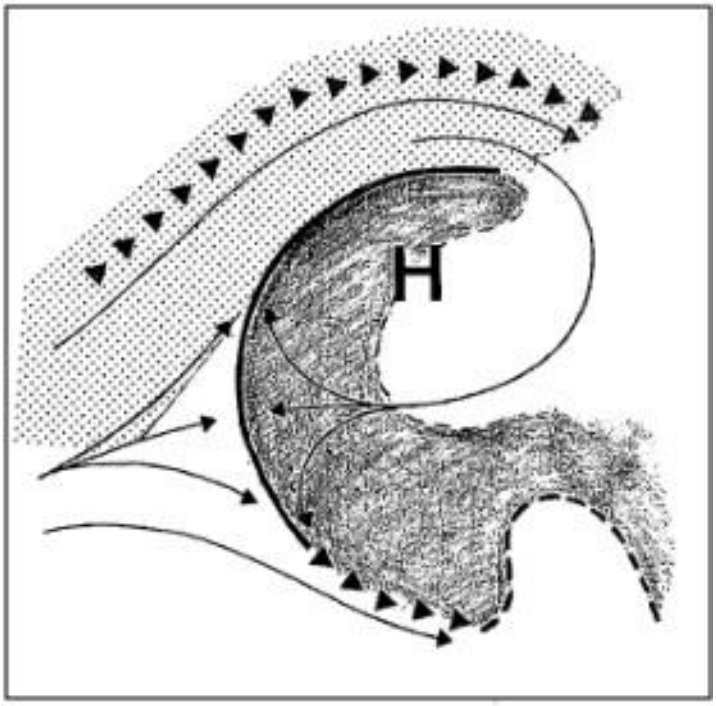

Fig. 4-2-9 Schematic illustration of an inside boundary. Shading: dark region; white: bright region; dotted area: cloud; thick line: boundary; thin arrows: streamlines; black triangles: axis of maximum wind speed.

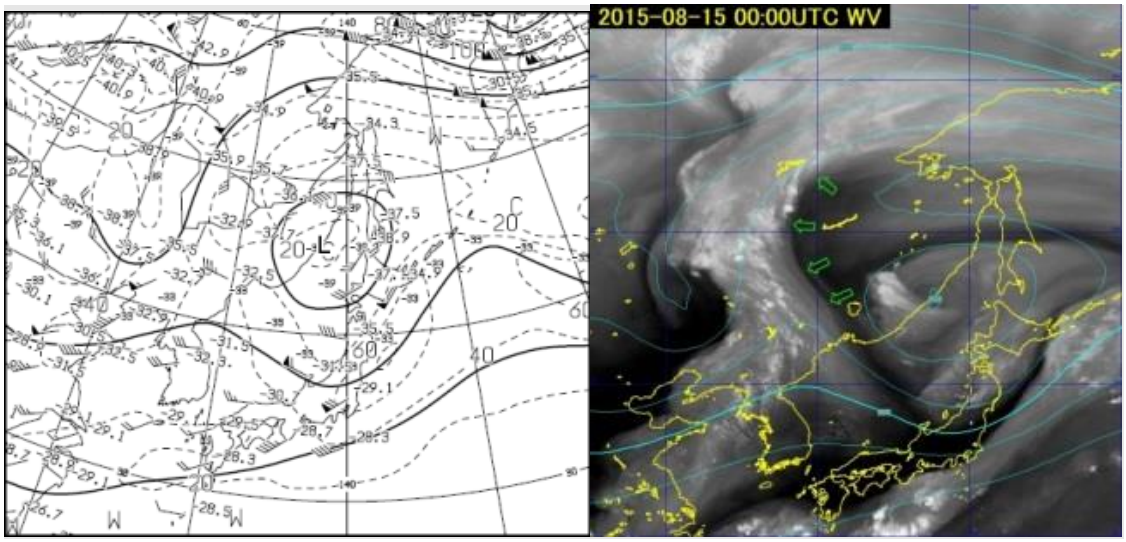

Fig. 4-2-10 Inside boundary for 00:00 UTC on 15 August 2015. Left: 300 hPa weather chart; right: water vapor image; green arrows: boundary, cyan lines: 300 hPa contour line from GSM.

4.2.3. Boundaries Exhibiting a Surge

In water vapor imagery, dark regions rushing in from upstream are called surges. Boundaries formed by such regions and bright regions at the front in the direction of movement

are called surge boundaries, which can be divided into dry surge boundaries (where the dark region extends in a convex manner eastward) and base surge boundaries (where the dark region extends in a convex manner toward the equator). Surge boundaries provide important information in analysis of water vapor imagery because they promote convective activity and contribute to the generation of turbulence due to the presence of dry air masses in the upper layer.

4.2.3.1. Dry Surge Boundaries

Cold air mass advection in the upper and middle layers, deceleration downstream of the jet core, and subsidence at the rear of developed cyclones are factors in downward stream development. Dark regions associated with downward streams form a clear boundary between the cloud area associated with the cyclone in front, known as a dry surge boundary. As per Fig. 4-2-11, the dark region moves in a convex manner downstream and the boundary moves rapidly.

When there is a warm and humid air mass in the lower layer near the dry surge boundary, an associated dry air mass in the upper layer flows in and promotes instability, necessitating caution for convective cloud development. Disturbances such as clear air turbulence (CAT) are likely to emerge between this boundary and the dark region on the upstream side (Ikeda and Okumura, 1999).

Figure 4-2-12 shows a dry surge boundary. The tip of the dark region moving eastward from near Primorye has reached the sea east of Hokkaido, forming a boundary at the rear of the trough extending over the Sea of Okhotsk to the area east of Japan. This is a dry air mass accompanied by a cold air mass moving quickly eastward with increasing darkness, indicating a strong downward stream in the deceleration area behind the trough.

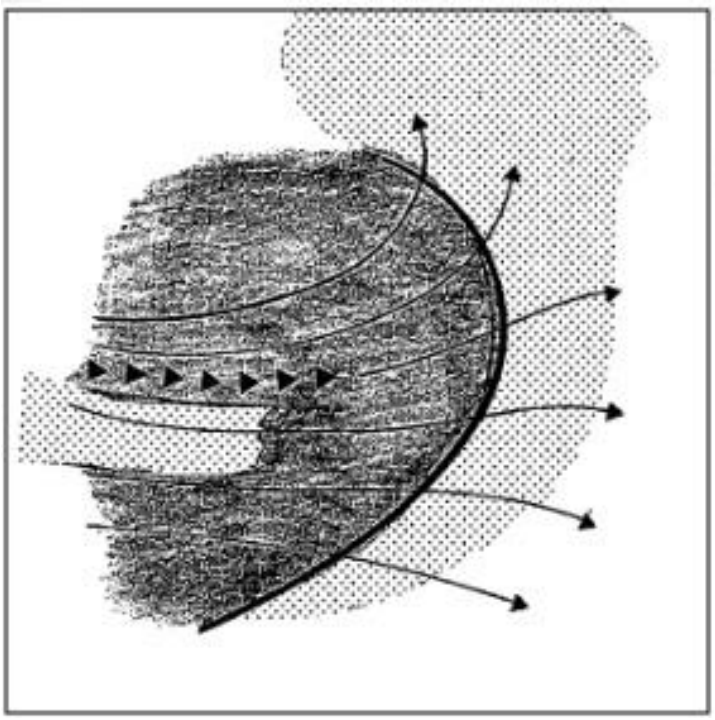

Fig. 4-2-11 Schematic illustration of a dry surge boundary. Shading: dark region; white: bright region; dotted: cloud; thick line: boundary; arrows: streamlines; black triangles: axis of maximum wind speed.

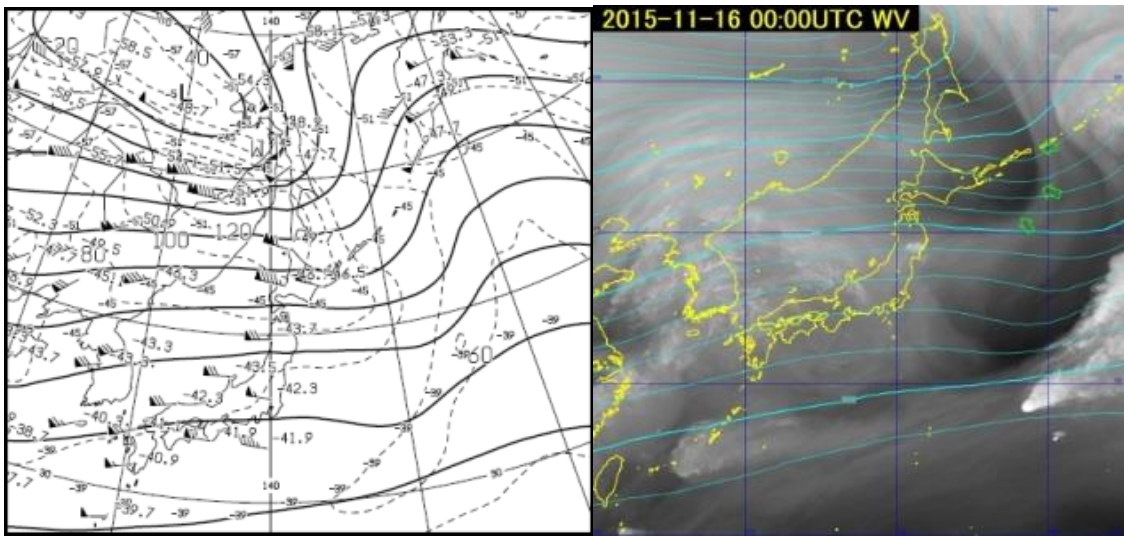

Fig. 4-2-12 Dry surge boundary for 00:00 UTC on 16 November 2015. Left: 300 hPa weather chart; right: water vapor image; green arrows: boundary, cyan lines: 300 hPa contour line from GSM.

4.2.3.2. Base Surge Boundaries

Due to upper-ridge strengthening, northerly winds fortify to the east of the ridge and the dry air mass moves southward, forming a base surge boundary between itself and the humid

air mass on the tropical side. Boundaries usually appear as narrow strips, but in Fig. 4-2-13 a dark region representing a base surge boundary expands southward. Similar to the situation with dry surge boundaries, forms of turbulence such as CAT tend to occur between such boundaries and dark regions upstream (Ikeda and Okumura, 1999). Base surge boundaries may move southward to the Intertropical Convergence Zone (ITCZ) and activate convection. Especially in the tropics, monitoring of such boundaries is important in the generation and development of convective systems.

Figure 4-2-14 shows a base surge boundary formed between a dry air mass (dark region) moving southward from a ridge developing near Japan and a moist air mass to the south (bright region).

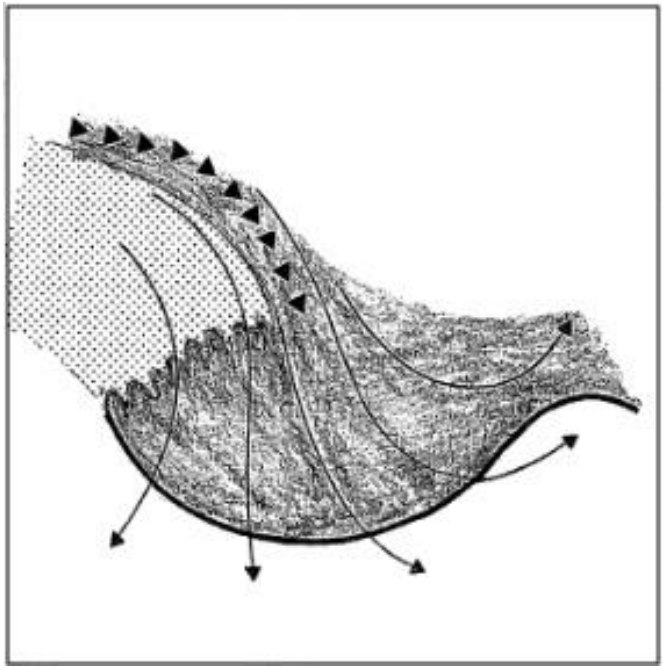

Fig. 4-2-13 Schematic illustration of a base surge boundary. Shading: dark region; white: bright region; dotted area: cloud; thick line: boundary; thin arrows: streamlines; black triangles: axis of maximum wind speed.

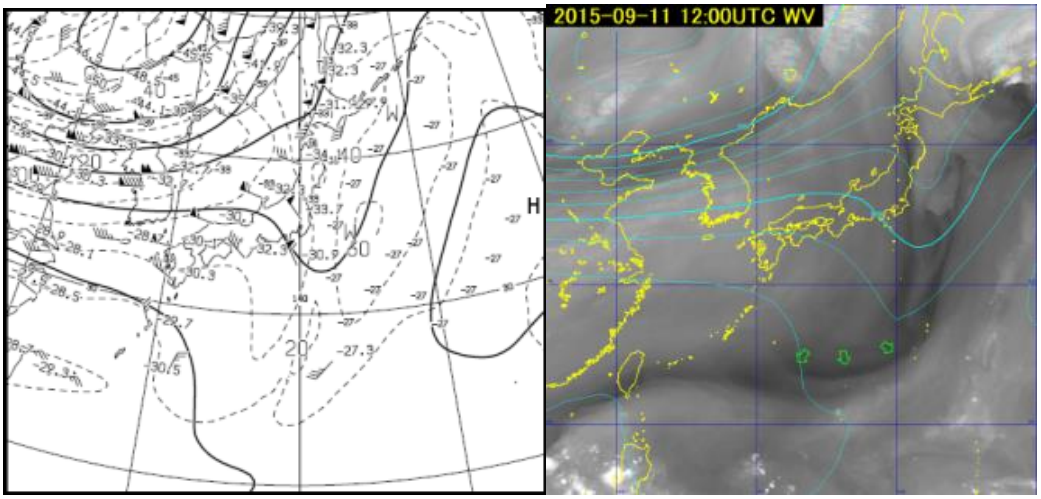

Fig. 4-2-14 Base surge boundary for 12:00 UTC on 11 September 2015. Left: 300 hPa weather chart; right: water vapor image; green arrows: boundary, cyan lines: 300 hPa contour line from GSM.

4.2.4. Others

4.2.4.1. Return Moisture Boundaries

In Fig. 4-2-15, a return moisture boundary is seen on the eastern side of an upper ridge between a moist air mass (bright region) moving southward and a dry area (dark region). This formed due to a upper-level moist air mass flowing toward the equator with no influence from synoptic-scale vertical motion. The name “return moisture boundary” reflects how moisture moving northward in front of the trough crosses over the ridge and returns toward the equator. Such boundaries have a bright/dark pattern opposite to that of base surge boundaries in water vapor images, but are not related to downward streams and do not correspond to significant weather disturbances such as fronts and cyclones.

Figure 4-2-16 shows a return moisture boundary formed between a bright region in a convex form toward the equator, extending from the area east of Japan to the area far east of Japan, and a dark region on the polar side of the jet stream extending from Primorye to the area far east of Japan.

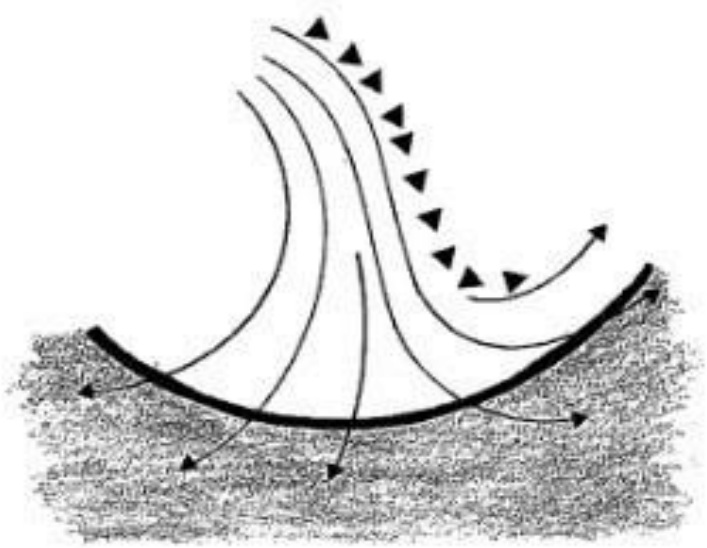

Fig. 4-2-15 Schematic illustration of a return moisture boundary. Shading: dark region; white: bright region; thick line: boundary; thin arrows: streamlines; black triangles: axis of maximum wind speed.

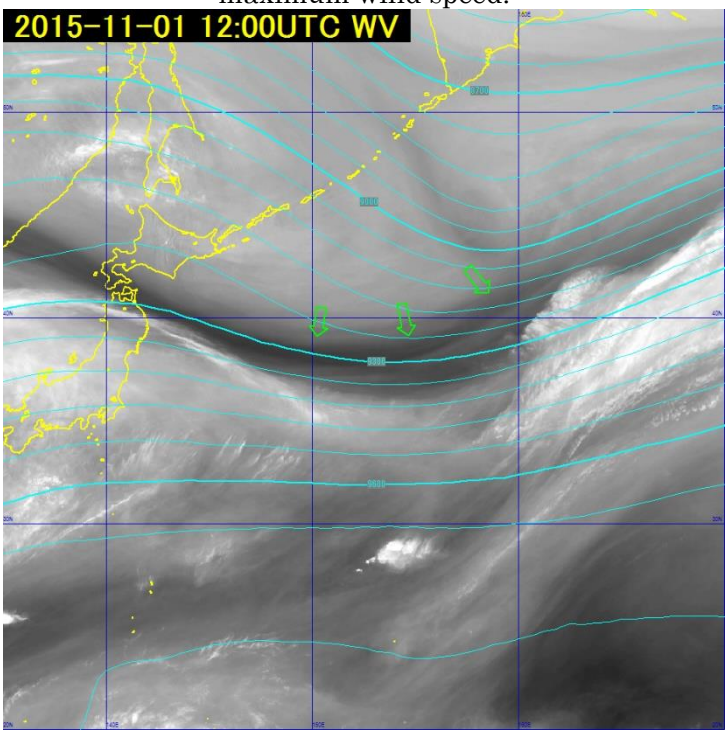

Fig. 4-2-16 Water vapor image for 12:00 UTC on 1 November 2015, showing a return moisture boundary (green arrows).

Reference

- Ramond *et al.,* 1981: The Dynamics of Polar Jet Streams as Depicted by the METEOSAT WV Channel Radiance Field, Monthly Weather Review, 109, 2164-2176.
- Weldon and Holmes, 1991: Water Vapor Imagery, NOAA Technical Report NESDIS 57.

4.3. Analysis Using Water Vapor Imagery

4.3.1. Cold Lows

Upper vortices are visualized in patterns in water vapor imagery, allowing analysis and tracking even in the absence of clouds. These often correspond to cold lows.

Figures 4-3-1 and 4-3-2 show water vapor images for an upper vortex moving eastward from the sea near the Kuril Islands. 500 hPa weather charts (Figs. 4-3-3 and 4-3-4) show that the center of the upper vortex and the cold low largely coincide.

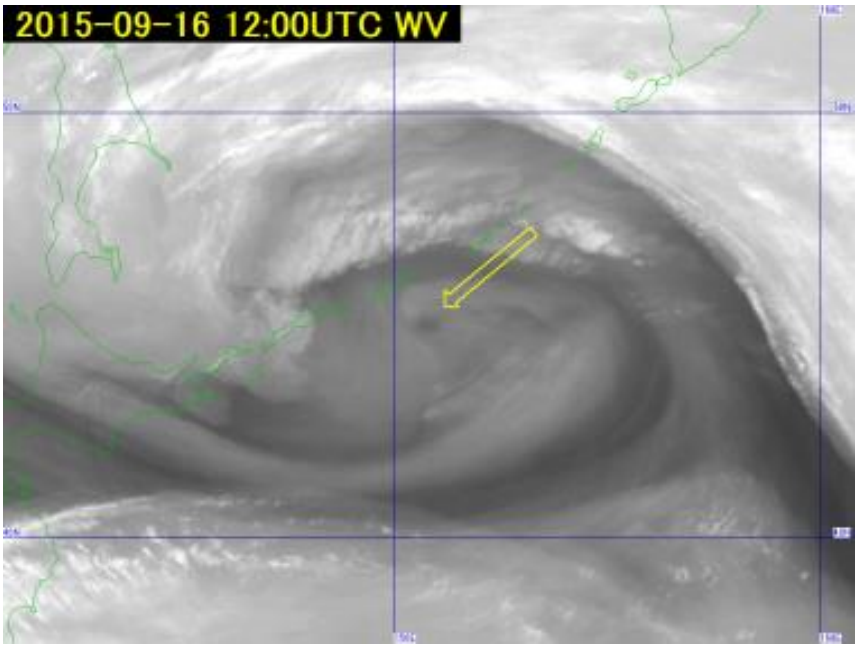

Fig. 4-3-1 Water vapor image of a cold low for 12:00 UTC on 16 September 2015

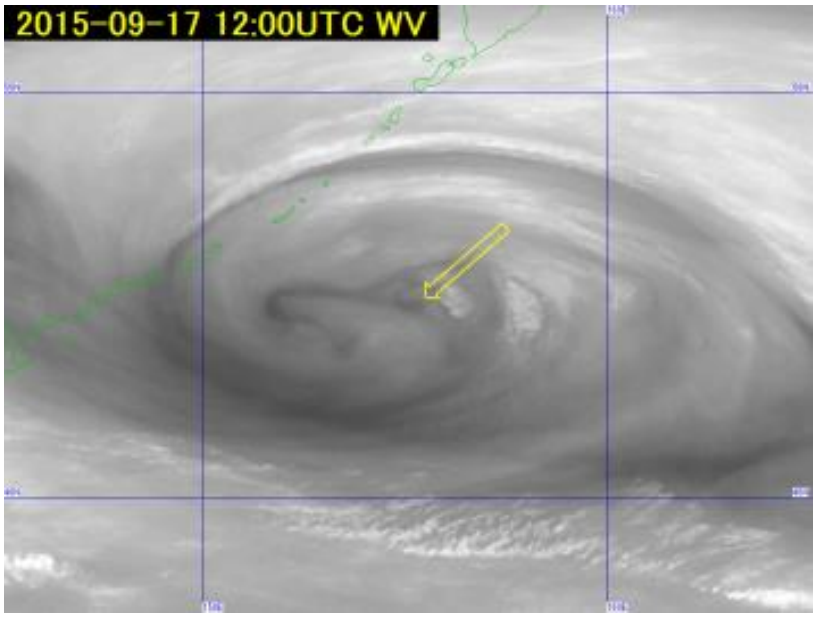

Fig. 4-3-2 Water vapor image of a cold low for 12:00 UTC on 17 September 2015

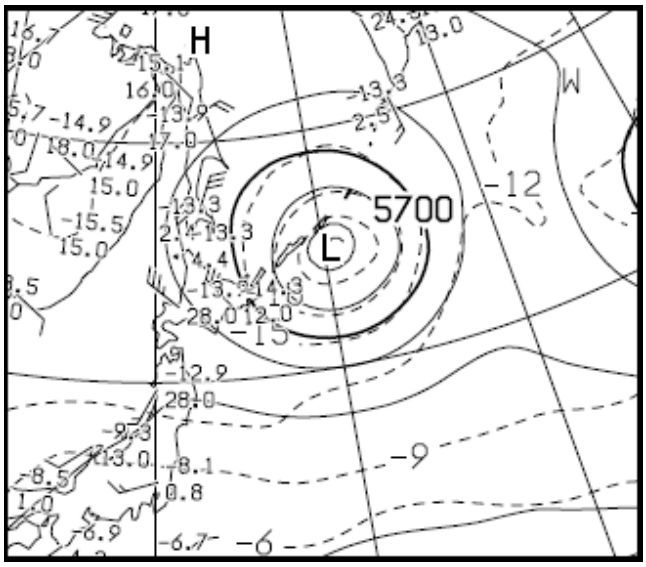

Fig. 4-3-3 500 hPa weather chart for 12:00 UTC on 16 September 2015

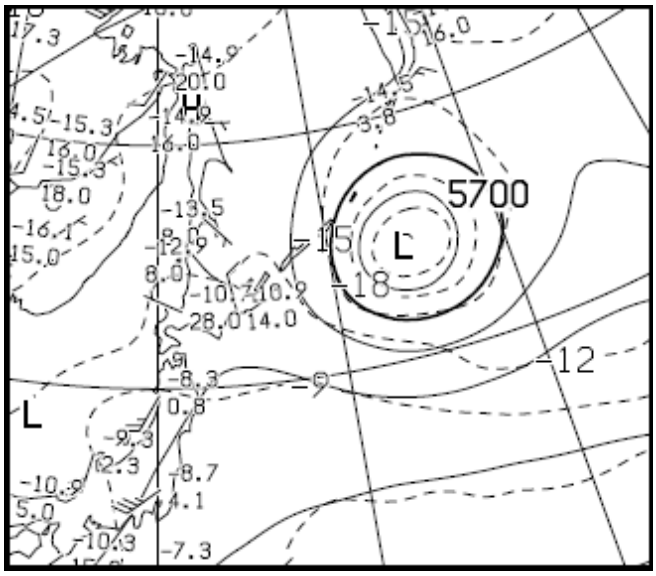

Fig. 4-3-4 500 hPa weather chart for 12:00 UTC on 17 September 2015

4.3.2. Upper Cold Lows (UCLs)

Shimamura (1981) refers to cold low-type cyclonic circulation analyzed in tropical and subtropical regions as an upper cold low (UCL), with the following notations:

1. Early UCL stages often feature a humid area to the east of the center and a dry area near/westward of the center in correspondence with the cloud area.
2. Convective clouds are active around the UCL, and the surrounding area may develop typhoon conditions.

Naito (1993) and Takamine (1995) state that UCLs are often observed along tropical upper

tropospheric troughs (TUTTs), which are formed by streams descending southward from the upper layer near Japan and streams moving northward while sinking from the upper layer of ITCZ. Thus, it is important to track UCLs in monitoring of tropical disturbances.

Figure 4-3-5 shows a water vapor image for a clearly identifiable upper vortex corresponding to a UCL moving westward from Wake Island (green arrow). The 250 hPa weather chart (Fig. 4-3-6) shows the vortex and cyclone centers almost at the same location. The minimum cold value **C** (abbreviation for cold; the local minimum point of temperature) is just to the north of **L** on the weather map, indicating that the temperature around the upper vortex is lower than in the surrounding area. Although not prominent here, convective cloud areas containing Cb tend to emerge and develop around vortices due to the presence of upper cold air. Cold lows in the westerly wind belt generally move southward or eastward, whereas UCLs separated from the westerly wind belt sometimes approach Japan while moving northward or westward over southern and eastern sea areas.

Meanwhile, a clear vortex is seen over the sea near Chichijima (red arrow) in association with a typhoon, rather than being a UCL. The major difference from a UCL is that the upper layer near the center is accompanied by warm air **W** rather than cold air **C**, as seen on the 250 hPa weather chart.

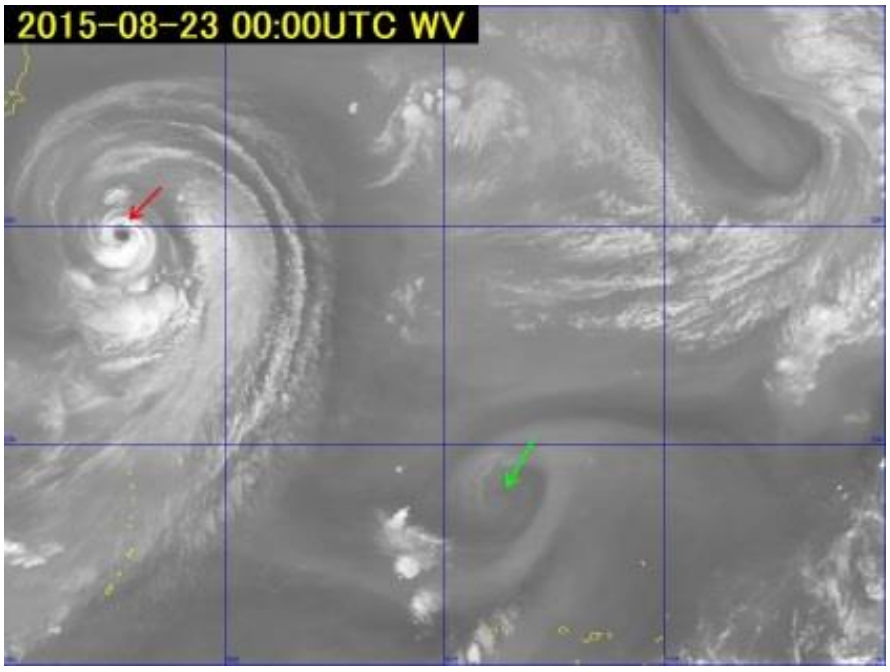

Fig. 4-3-5 Water vapor image of UCL for 00:00 UTC on 23 August 2015

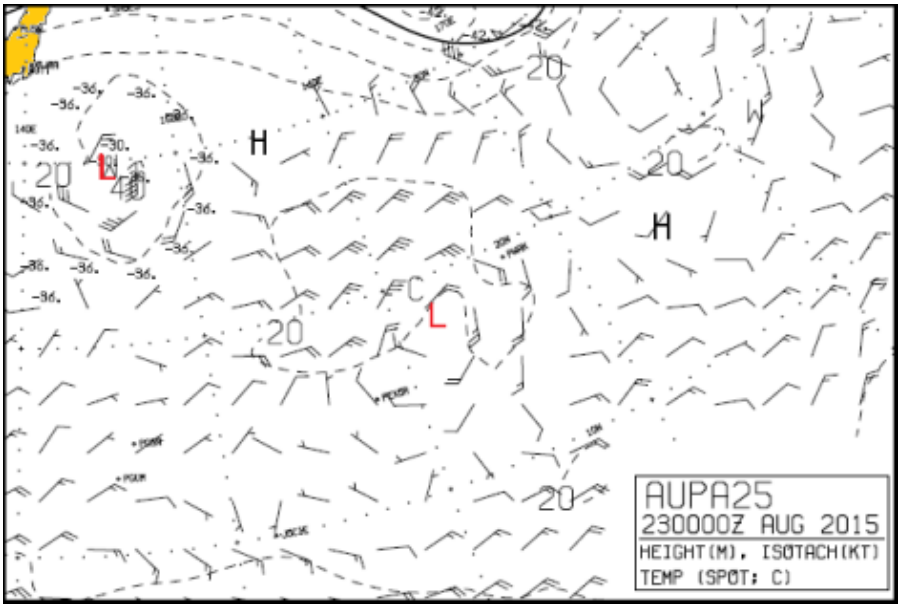

Fig. 4-3-6 250 hPa weather chart for 00:00 UTC on 23 August 2015

4.3.3. Promotion of Convective Activity

An inflow of dry air mass (i.e., a low equivalent-temperature air mass) into the upper layer corresponds to deterioration of stability when the lower layer condition exhibits no change. When a dark region enters an area where convective clouds are present, stability deteriorates and convective activity is promoted. This is likely to occur at the front of the dark region in the direction of movement, and convection may turn active near the boundary. The dark region forming the surge boundary is often accompanied by cold air that increases instability, meaning that convective clouds are likely to develop.

Figures 4-3-7 and 4-3-8 show a dry surge boundary. The tip of the dark region moving eastward south of Japan forms a boundary behind a cloud area in a cyclone moving eastward south of Japan while occluding. This is a dry air mass with cold air, and a strong downward stream is seen behind the cyclone. Convective activity is limited at 12 UTC, but cumulonimbus (green arrows, Fig. 4.3.8) develops near the boundary at 18 UTC. These clouds were cumulus congestus and cumulus (green arrows on Fig. 4.3.7) six hours previously, and the dark region inflow appears to have promoted convective activity.

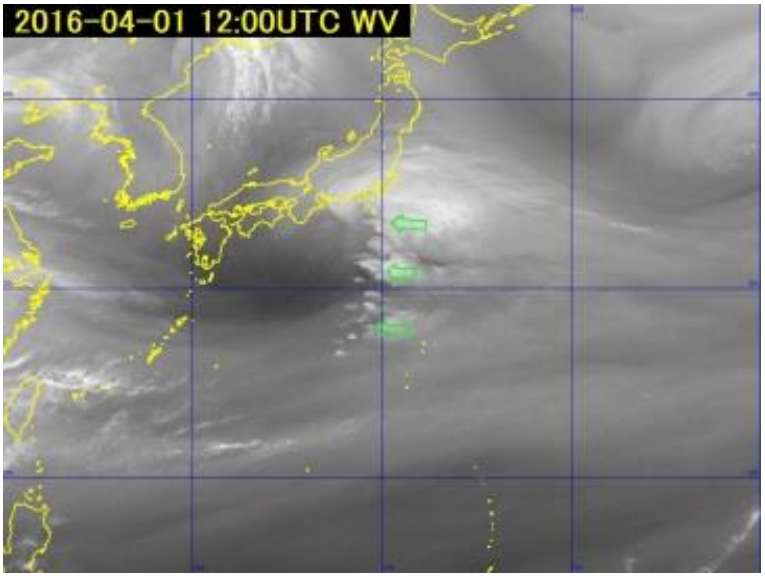

Fig. 4-3-7 Water vapor image for 12:00 UTC on 1 April 2016

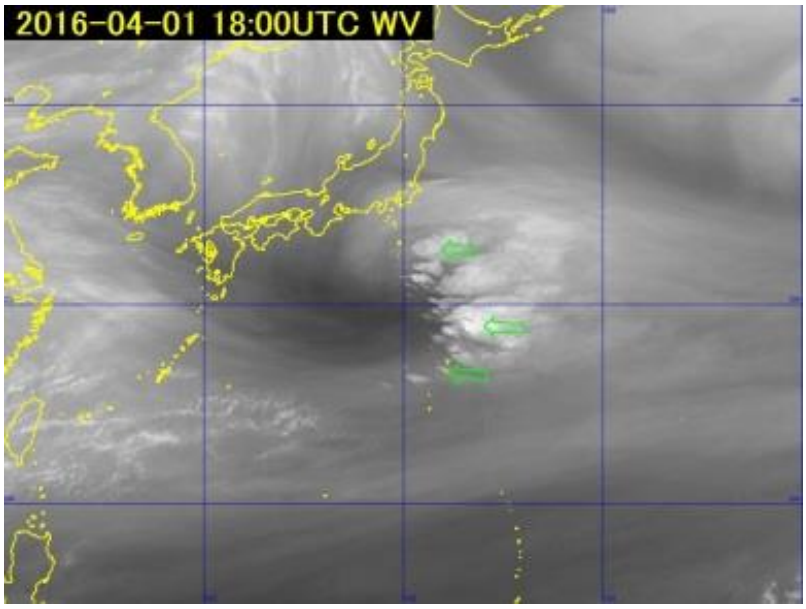

Fig. 4-3-8 Water vapor image for 18:00 UTC on 1 April 2016

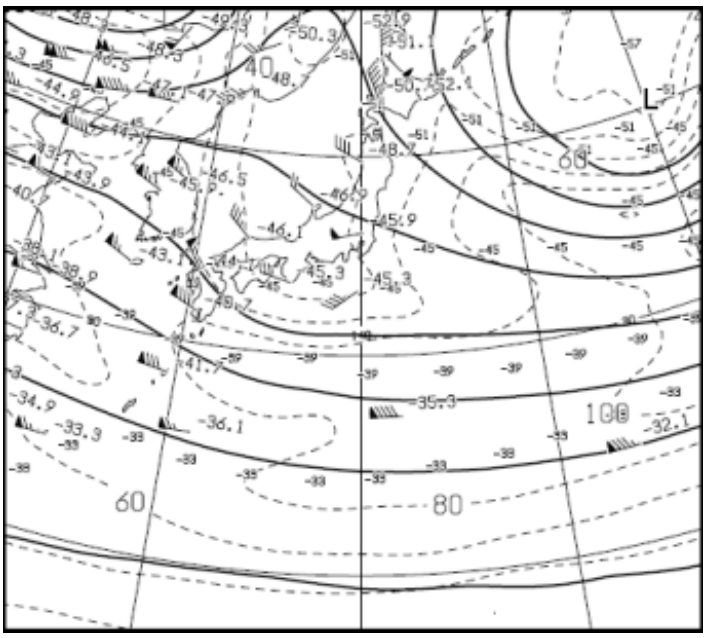

Fig. 4-3-9 300 hPa weather chart for 12:00 UTC 1 April 2016